REDVET - Revista electrónica de Veterinaria - ISSN 1695-7504
Vol 25, No. 1 (2024)
http://www.veterinaria.org
Article Received :Revised: Accepted:

In vitro efficacy of poly-gama-glutamic acid loaded nano-formulation of Levofloxacin and Moxifloxacin against Brucellosis.

Arijit Shil [1], Dr. Paramita Dey [2] , Dr. Pranabesh Chakraborty [3], Suman Mondal [4] , Tamalika Ray [5],Jayita Pal [6] Md Soyeb Mallick [7], Enakshi Ghosh [8], Souvik Ghosh [9], Disha Chattopadhyay [10].

[1]Arijit Shil, Faculty, Diploma in Veterinary Pharmacy, West Bengal University of Animal and Fishery Sciences, Government of West Bengal, Mohanpur Campus, Nadia, West Bengal, India.
[2]Dr. Paramita Dey, Professor, Department of Pharmaceutics, Bengal School of Technology, A College of Pharmacy, Chinsurah, Hooghly, West Bengal, India.
[3]Dr. Pranabesh Chakraborty, Former Director, Dept. of Food, Pharmaceutical & Health Care Technology. Maulana Abul Kalam Azad University of Technology, W.B.
[4]Suman Mondal, Master of Pharmacy, Department of Pharmacognosy, Bharat Technology, Uluberia, West Bengal, India
[5]Tamalika Ray , Assistant Professor, Department of Pharmacognosy, DmbH Institute of Medical Science, Dadpur, West Bengal.
[6]Jayita Pal, Master of Pharmacy, Department of Regulatory Affairs, Guru Nanak Institute of Pharmaceutical Science and Technology, Nilgunj Rd, Sahid Colony, Panihati, Khardaha, West Bengal
[7]Md Soyeb Mallick, Department of Pharmaceutics, Assistant Professor , Barasat Bidhan Chandra Roy Institute of Pharmacy ,Barbaria,Barasat,Duttapukur, North 24 PGS.
[8]Enakshi Ghosh ,Principal of Jiaganj Institute of Pharmacy , Amaipara , Jiaganj, Murshidabad
[9]Souvik Ghosh, Department of Pharmaceutics, Assistant Professor ,Gitanjali College of Pharmacy, Lohapur, Birbhum.
[10]Disha Chattopadhyay , Bachelor of pharmacy, Bengal college of Pharmaceutical Sciences & Research, Biplabi Reshbehari Sarani, Bidhannagar, Durgapur, West Bengal

Abstract
Background: Levofloxacin and Moxifloxacin are fluoroquinolone antibiotics used to treat brucellosis, caused by the Brucella bacteria. Typically, they are combined with other antibiotics for effective treatment, with selection depending on factors like the specific Brucella strain, patient health, and local antibiotic resistance.
Objective: The objective was to enhance the antibacterial activity of these fluoroquinolones by utilizing γ-PGA as a biocompatible nanocarrier. Nano-formulations were characterized for size, surface charge, and release profile. The antimicrobial activity was assessed using standard microbiological assays, demonstrating improved potency and extended release.
Methods: The double emulsion-synthesized levofloxacin/moxifloxacin-encapsulated nanoparticles were characterized using Dynamic Light Scattering (DLS), Fourier Transform Infrared Spectroscopy (FTIR), and Scanning Electron Microscopy (SEM).
Results: The results indicate that the γ-PGA-based nano-formulations of levofloxacin and moxifloxacin show promising in vitro efficacy, offering potential for more effective treatment strategies for brucellosis.
Conclusion: According to the results study demonstrated that LEV/MOX-loaded nanoparticles (NPs) are more effective than free drugs in combating Brucella melitensis phagocytosed by macrophages.

Keywords: Levofloxacin, Moxifloxacin, Nanoparticles, Targeted drug delivery system, Brucella treatment

[*]**Corresponding Author:** Arijit Shil
[*]Faculty, Diploma in Veterinary Pharmacy. West Bengal University of Animal and Fishery Sciences, Government of West Bengal, Mohanpur, Nadia, Email- amearijit1000@gmail.com

INTRODUCTION:

Brucellosis is a bacterial zoonotic disease caused by the Brucella genus, affecting both animals and humans through contact with infected livestock or consumption of contaminated products. The bacteria are small, gram-negative, and survive inside host cells. Key human-infecting species include Brucella melitensis (from sheep and goats), Brucella abortus (from cattle), Brucella suis (from pigs), and Brucella canis (from dogs). The disease is widespread, especially in areas with intensive livestock farming [1].

REDVET - Revista electrónica de Veterinaria - ISSN 1695-7504
Vol 25, No. 1 (2024)
http://www.veterinaria.org
Article Received :Revised: Accepted:

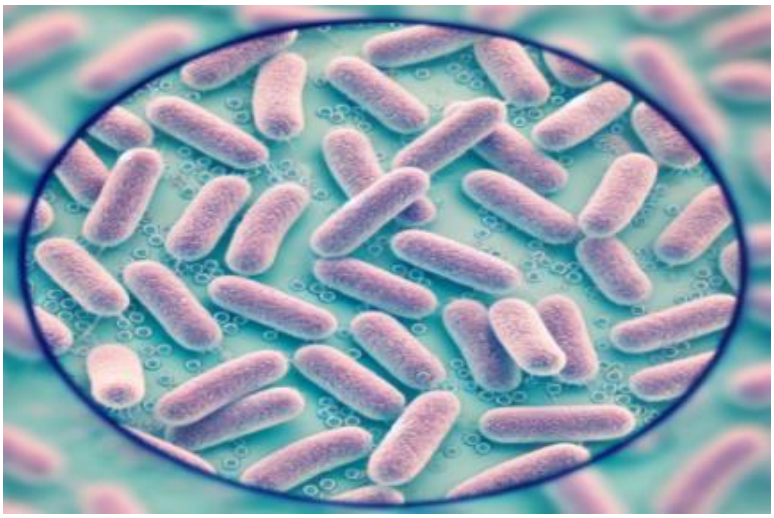

Fig 1: Zoonotic Brucella Bacteria

Transmission:
Brucellosis mainly spreads to humans via contact with infected animals or consumption of contaminated dairy products. Rarely, it can be transmitted through inhalation of bacteria, posing a risk to farmers and lab workers. Human-to-human transmission is extremely uncommon [2].

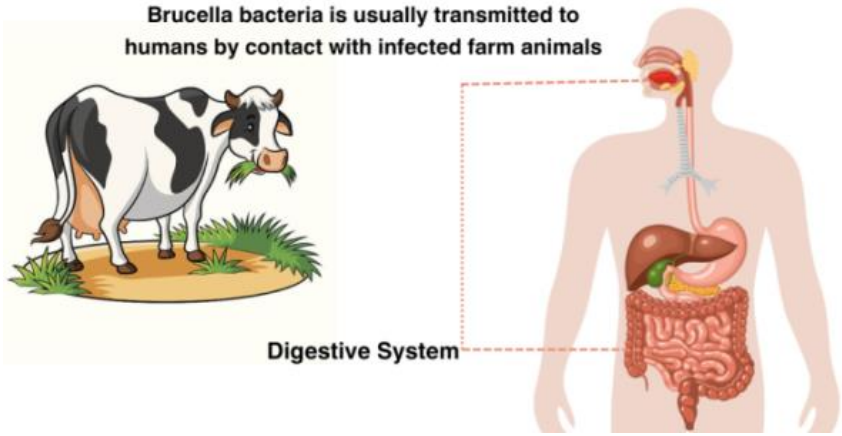

Fig 2: Transmission of Brucella Bacteria; animal to human

Treatment:
Brucellosis treatment requires a combination of antibiotics to eliminate the bacteria, especially since it can survive inside host cells. Standard therapy includes doxycycline (100 mg twice daily) and rifampicin (600-900 mg daily) for six weeks. Severe cases may need additional antibiotics like streptomycin or gentamicin. Complications such as neurobrucellosis or endocarditis require extended treatment, often using doxycycline, rifampicin, and ceftriaxone for at least six months. For bone and joint infections, therapy may last up to 12 weeks, potentially including fluoroquinolones. During pregnancy, safer alternatives like rifampicin and trimethoprim-sulfamethoxazole are used, as doxycycline can harm the fetus. Children typically receive trimethoprim-sulfamethoxazole and rifampicin [3].

Activity of Fluoroquinolones Against Brucella Bacteria:
Fluoroquinolones are a class of antibiotics with broad-spectrum activity that have shown effectiveness in treating Brucella infections (brucellosis), though they are not typically the first-line treatment. Their use in the management of brucellosis has been explored, particularly in cases of resistance to standard treatments or when conventional therapy is contraindicated [4].

Mechanism of Action:
Fluoroquinolones work by inhibiting bacterial DNA gyrase and topoisomerase IV, enzymes essential for bacterial DNA replication, transcription, and repair. This mechanism leads to the death of the bacterial cell. In the case of Brucella

bacteria, fluoroquinolones can penetrate intracellular environments, which is crucial for treating intracellular pathogens like Brucella that survive and replicate inside macrophages [5].

Use of Fluoroquinolones against Brucellosis:
Fluoroquinolones like ciprofloxacin and ofloxacin are often combined with rifampin or doxycycline for brucellosis treatment to reduce relapse risk seen with single-drug use. Ciprofloxacin alone has shown moderate success but is linked to high relapse rates, necessitating combination therapy for better results. These antibiotics effectively penetrate cells, targeting Brucella bacteria residing within macrophages. This intracellular action is crucial as Brucella species can survive inside host cells. Thus, fluoroquinolones are valuable in chronic or relapsed cases, particularly when combined with doxycycline or rifampin. Studies suggest their effectiveness improves when used in combination regimens [6].

MATERIALS AND METHODS

MATERIALS, INSTRUMENTS, SOFTWARE

The successful formulation and development of a dosage form depend on the precise selection of active pharmaceutical ingredients and excipients that are compatible within the medicinal product. In this study, PGA was employed as the foundational polymer for the preparation of polymeric nanoparticles. Alongside the polymer, a comprehensive list of chemicals, reagents, and active pharmaceutical ingredients utilized in the formulation is provided below. Additionally, detailed information on these has been included in the for reference in future work.

Materials
Levofloxacin (From macleods Pharma Sikkim), Moxifloxacin (From macleods Pharma Sikkim), , Poly-gama-glutamic acid (PGA) (Cyben Biotech, East China) , Ethyl acetate , Ethanol, Tween 80, Methanol,

Instruments
Digital pH meter, Digital Melting Point Apparatus, Analytical Balance, UV-spectrophotometer, Dissolution Tester, X-ray Diffractometer, Hot Air Oven, Particle Size Analyzer, Freeze Dryer.

Software used in present investigation
Design Expert Software 8.0.7.1

Formulation Technique of Nanoparticles
The creation of nanoparticles presents significant challenges in the formulation industry. Various methods have been developed to dissolve, entrap, adsorb, attach, or encapsulate the active pharmaceutical ingredient (API) within or onto a nanosized matrix. Nanospheres and nanocapsules, while similar in size, are designed for distinct applications. The physical structure of nanoparticles is influenced by the formulation techniques used, which ultimately affect the drug release characteristics from the nanoparticles [4].

Preparation of Primary and Secondary Water Phases
To prepare the formulation, a precise amount of poly gama glutamic acid (PGA) was weighed and placed in a 150 ml glass beaker. The crystalline PGA was then wetted with a specific volume of deionized water and left to soak for 20-30 minutes while continuously stirring at 500 rpm using a magnetic stirrer. Following this, the temperature was raised to 50°C to enhance the dissolution process until a clear PGA solution was achieved [7]. This clear solution indicates a uniform stock solution of PGA, which was subsequently used. The primary (w1) and secondary (w2) water phases of the emulsion were prepared by diluting the stock solution with deionized water in various ratios [8].

Double Emulsion Solvent Evaporation Technique
The double emulsion solvent evaporation technique is a widely adopted method for encapsulating various drug types within a multi-compartmental structure. This process generally includes two common types of double emulsions: water-oil-water (w/o/w) and oil-water-oil (o/w/o). These two-step processes are frequently utilized to encapsulate both lipophilic and hydrophilic drugs in different compartments of the emulsion droplet. In this study, a w/o/w emulsion was prepared to achieve the primary objectives [9].
Initially, a single emulsion (w1/o) was formed by dispersing the inner aqueous phase (w1) into the oil phase. This was followed by the dispersion of the primary emulsion (w1/o) into a larger volume of the outer aqueous phase (w2). Both aqueous phases were formulated with emulsifiers at varying concentrations to stabilize the double emulsion (8). A modified double emulsion solvent evaporation technique (w1/o/w2) was used to prepare polymeric nanoparticles, with levofloxacin/moxifloxacin as the model drug. For this preparation, accurately weighed PGA (50 mg) and levofloxacin/moxifloxacin (20 mg) were dissolved in a total of 2 ml of an organic solvent system, divided into two separate Eppendorf tubes. The solvents were carefully selected for creating the polymer-drug mixture as the oil phase [10].

REDVET - Revista electrónica de Veterinaria - ISSN 1695-7504
Vol 25, No. 1 (2024)
http://www.veterinaria.org
Article Received :Revised: Accepted:

The primary water phase (w1) was emulsified with the oil phase through dropwise addition, using high-speed homogenization at 26,000 rpm for 5 minutes. Subsequently, the primary emulsion (w1/o) was added to the secondary water phase (w2), containing 0.5% PGA, while maintaining a homogenization speed of 8,000 rpm. The prepared w/o/w emulsion was then sonicated at 20°C for 30 minutes. After sonication, the emulsion was left to stir overnight (10 hours) at 330 rpm to facilitate the evaporation of the organic solvents [11].

Collection and Lyophilization of Nanoparticles

As the organic solvent evaporated, the soft polymeric droplets transitioned into solid particles. The double emulsion was stirred at a low RPM (330 rpm) for an extended period to ensure the individual solidification of the nanodroplets. At this stage, the mixture was referred to as a nanosuspension, allowing for the easy removal of solid particles from the secondary water phase (w2) via centrifugation. A centrifugal force of 28,672 g was applied to facilitate the collection of all particles, correlating sedimentation rate with applied force [12]. The suspension was centrifuged at 18,000 rpm for 30 minutes at 5°C. After removing the supernatant liquid (w2), the nanoparticles were collected at the bottom of the centrifuge tube as a pellet. This pellet was then disaggregated through sonication (0.5-1 minute, low amplitude) in deionized water and re-collected by centrifugation at the same speed for 10 minutes. This washing process was repeated three to four times to ensure complete removal of the surfactant (PVA) from the nanoparticles. Once the surfactant was fully eliminated, the solid polymeric particles were collected as an aqueous concentrate of nanosuspension (2 ml) and transferred to a petri dish. The nanosuspension was subsequently stored at –60°C in a lyophilizer for freeze-drying until all water was removed from the nanoparticles [13].

RESULT AND DISCUSSION:

Determination of organic solvent and solubility

Nano-emulsions are biphasic systems of oil and water phases, stabilized using polymeric nanoparticles via the double emulsion solvent evaporation method. Drug solubility, a key factor in stability, was optimized using a mixture of ethyl acetate and ethanol. A 5:3 ethyl acetate-ethanol ratio improved Levofloxacin/moxifloxacin solubility, reducing crystal formation compared to ethyl acetate alone. The study found that an 8:2 or 5:3 ratio provided the best solubilizing properties, with 50:30 (ethyl acetate:ethanol) achieving the highest solubility. All formulations used this solvent mix to assess impacts on various parameters [14].

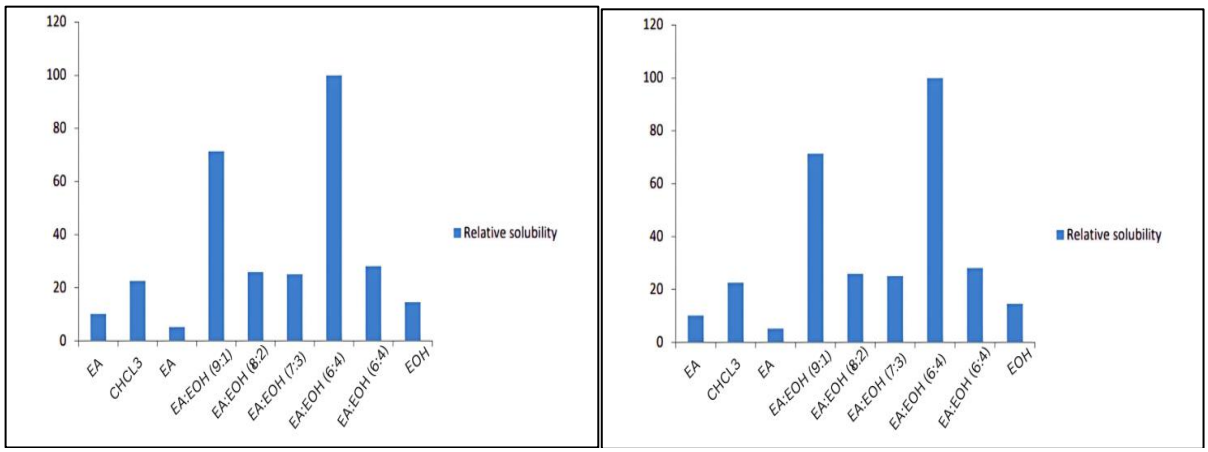

Figure 3: Relative solubility of levofloxacin/moxifloxacin in different organic solvents with same conc.

Determination of Crystallinity

The presence of crystalline active pharmaceutical ingredients (APIs) can greatly affect the distribution of the drug within a polymer matrix, potentially reducing the therapeutic effectiveness of the dosage form. One approach that has gained considerable attention for improving drug dissolution is solid dispersion (SD) using hydrophilic polymers [15].

REDVET - Revista electrónica de Veterinaria - ISSN 1695-7504
Vol 25, No. 1 (2024)
http://www.veterinaria.org
Article Received :Revised: Accepted:

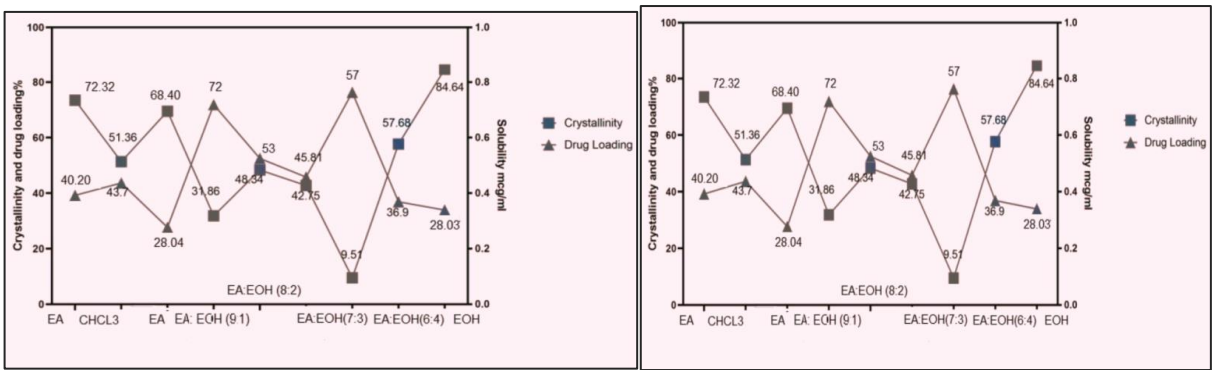

Figure 4: A comparative graphical representation of crystallinity and drug loading of lev and mox.

Solid phase characterization of drug and excipients

FTIR study

The compatibility of Levofloxacin and excipients was evaluated using Fourier Transform Infrared (FTIR) spectroscopy on a physical mixture of all components. FTIR spectra were recorded from 3600 cm^{-1} to 400 cm^{-1}, revealing characteristic peaks for Levofloxacin at 1892.36 cm^{-1} (aromatic C-H stretching), 1455.40 cm^{-1} (aliphatic C-H stretching), and 1315.90 cm^{-1} (C=C bond in aromatic rings). PGA displayed notable peaks at 1916.73 cm^{-1} (C=O stretching) and 1841.65 cm^{-1} (C-H stretching). The FTIR spectrum of the physical mixture showed no new peaks, indicating that no significant chemical interactions occurred between the drug and excipients [16].

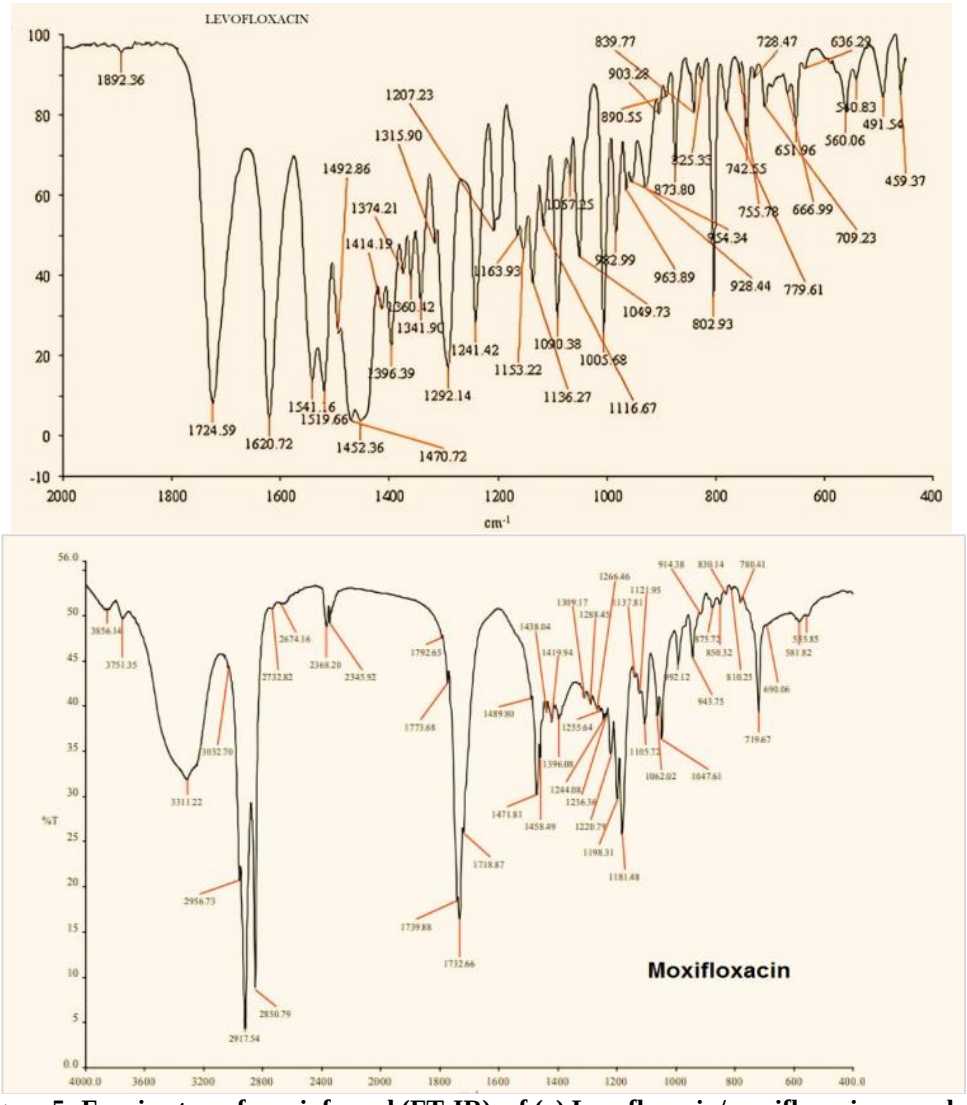

Figure 5: Fourier-transform infrared (FT-IR) of (a) Levofloxacin/moxifloxacin pure drug

REDVET - Revista electrónica de Veterinaria - ISSN 1695-7504
Vol 25, No. 1 (2024)
http://www.veterinaria.org
Article Received :Revised: Accepted:

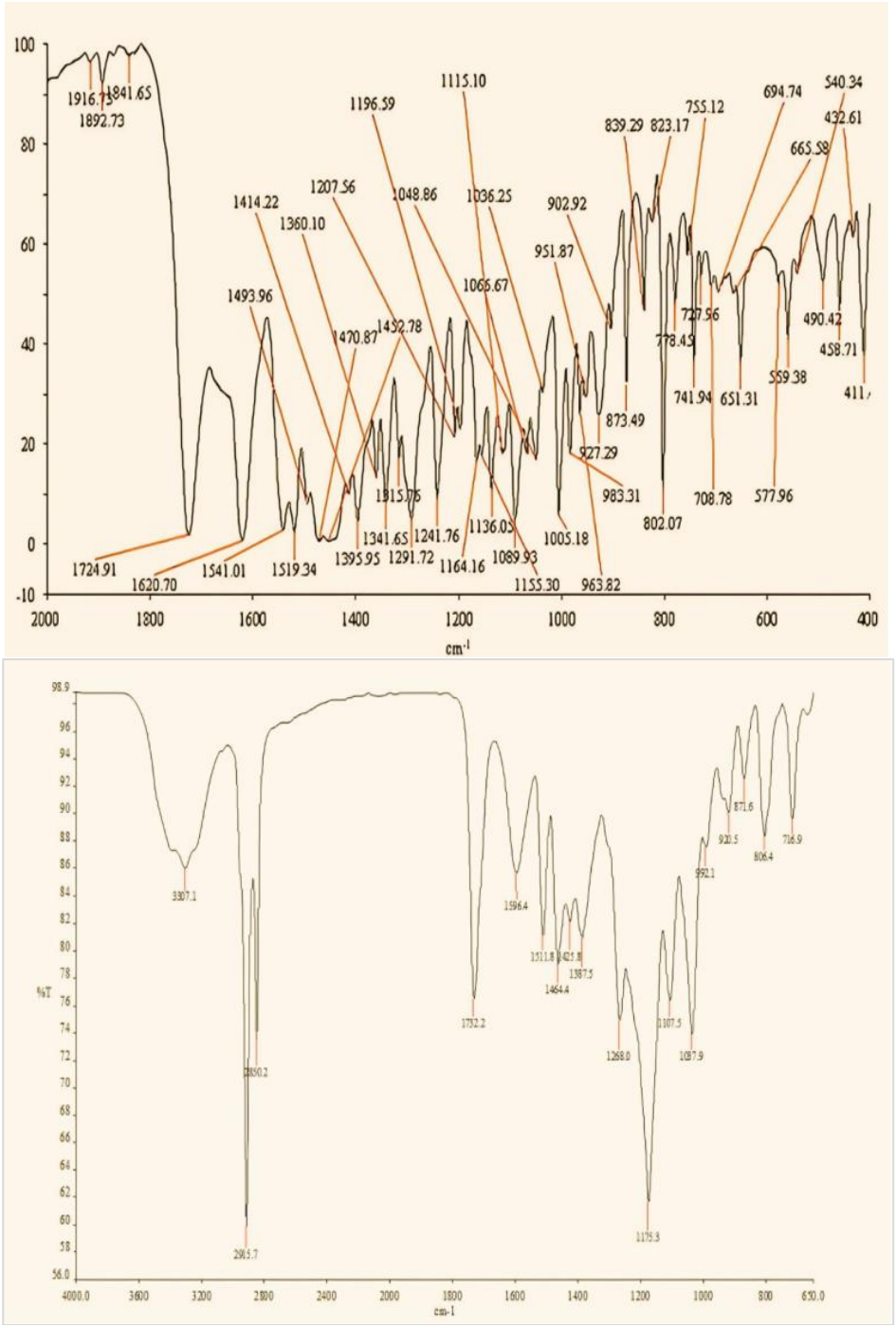

Figure 6: Fourier-transform infrared (FT-IR) spectra of Levofloxacin/moxifloxacin and Poly (gama glutamic acid) mixture.

XRD study

Determining the physical form of materials is a crucial element in pre-formulation studies, as it can significantly affect the formulation of drug-loaded nanoparticles and their release profiles. To assess the physical properties of the samples, X-ray diffraction (XRD) analysis was performed on the drug, excipient (PGA), and blank nanoparticles. The XRD pattern of pure Levofloxacin displayed distinct diffraction peaks at 6.8°, 14.1°, 15.1°, and 22.2°, confirming its crystalline structure, with the peaks at 6.7°, 14.3°, and 22.3° being particularly prominent. The XRD pattern of pure Moxifloxacin displayed distinct diffraction peaks at 6.7°, 14.1°, 15.1°, and 22.2°, confirming its crystalline structure, with the peaks at 6.4°, 13.2°, and 22.3° being particularly prominent [17].

REDVET - Revista electrónica de Veterinaria - ISSN 1695-7504
Vol 25, No. 1 (2024)
http://www.veterinaria.org
Article Received :Revised: Accepted:

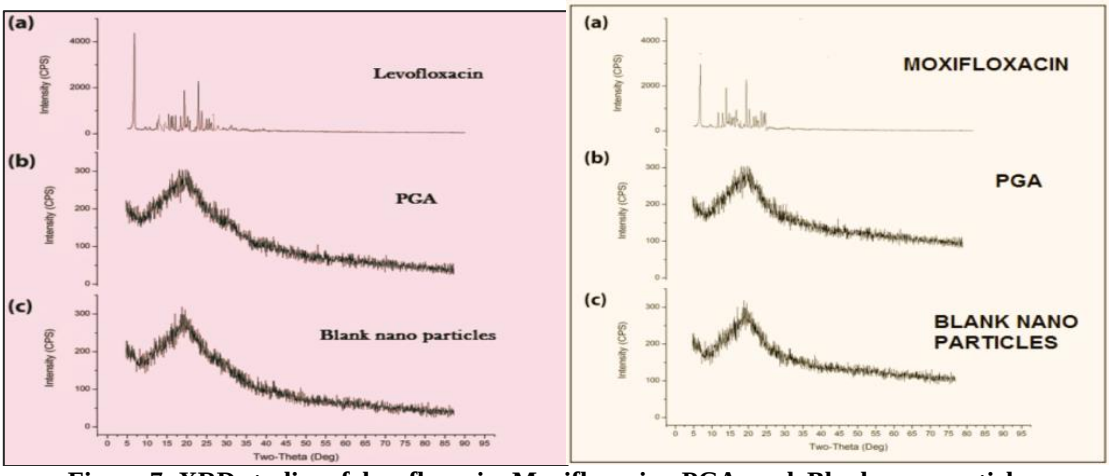

Figure 7: XRD studies of levofloxacin, Moxifloxacin , PGA and Blank nanoparticles.

DSC study

The thermograms of Levofloxacin, PGA, PVA, and their physical mixture are presented in , offering valuable insights into the thermal properties of these components and helping to identify any potential interactions between the drug and excipients in the solid state. Levofloxacin exhibited a distinct endothermic peak at 278.28°C, moxifloxacin exhibited a distinct endothermic peak at 282.34°C,which corresponds to its melting point and confirms its crystalline structure. In contrast, PGA showed an endothermic peak at 58.46°C, for mox PGA showed an endothermic peak at 54.32°C indicating its glass transition temperature and amorphous nature [18].

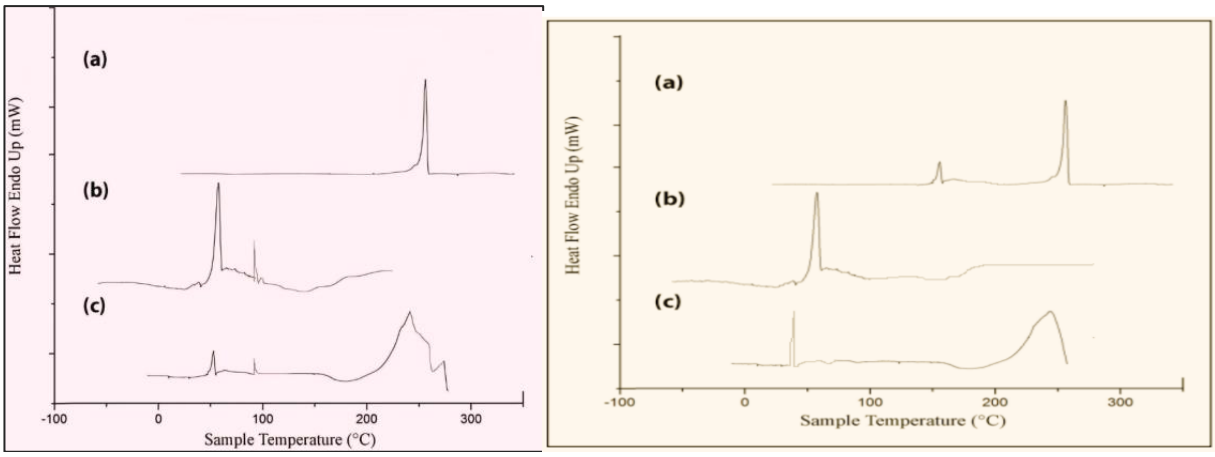

Figure 8 : DSC thermograms analysis of levofloxacin, moxifloxacin , PGA and Physical mixture.

Morphology of API and polymer

At 10KX magnification, the morphological analysis of pure Levofloxacin, moxifloxacin (API) revealed a heterogeneous geometric structure with solid particles of varying sizes, indicating a polydisperse distribution . In contrast, the SEM image of the polymer showed macromolecular formations without any defined particle size or shape, further confirming the amorphous nature of PGA [19].

REDVET - Revista electrónica de Veterinaria - ISSN 1695-7504
Vol 25, No. 1 (2024)
http://www.veterinaria.org
Article Received :Revised: Accepted:

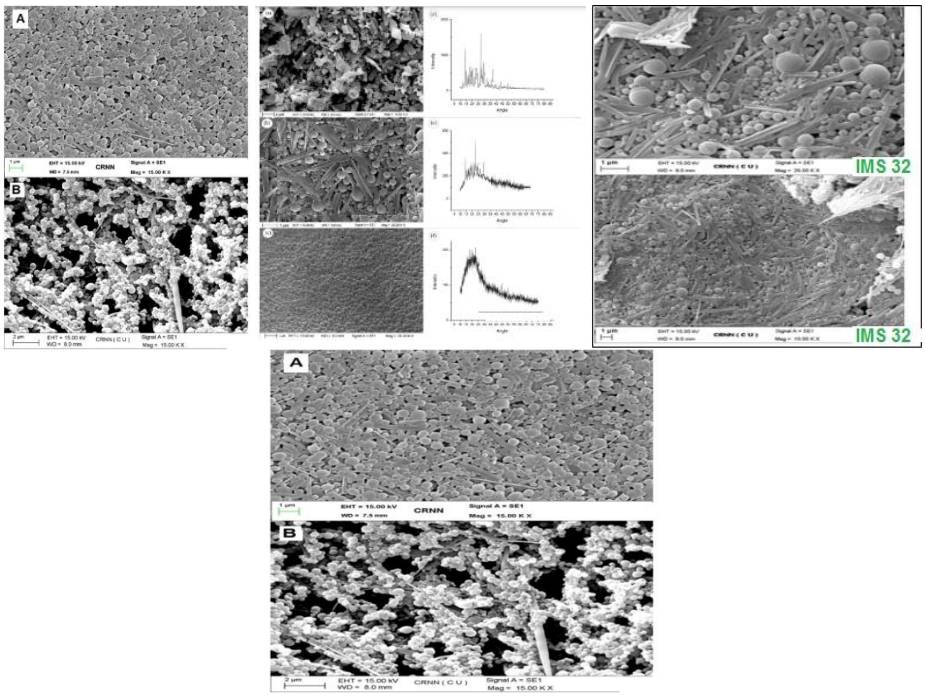

Figure 9: Morphological analysis of formulation

Formulation technique of polymeric NPs

In this study, a solubility-modulated double emulsion (W/O/W) solvent evaporation technique was employed to develop uniform, spherical drug-loaded polymeric nanoparticles (NPs). This advanced emulsification method facilitates the incorporation of two distinct compartments within a single nanodroplet. The appropriate concentration of polyvinyl alcohol (PVA) as the primary emulsifier stabilized the W/O emulsion, ensuring particle size consistency, which was subsequently reflected in the secondary W/O/W emulsion. High-speed homogenization reduced the primary emulsion droplets to nanoscale, followed by isolation at 27,144g to form W/O/W nanodroplets, resulting in a homogeneous secondary emulsion. To maintain nanodroplet mobility during nanoparticle formation, minimal mechanical stress (340 RPM) was applied [20]. The emulsion was magnetically stirred for 12 hours, allowing sufficient time for organic solvent evaporation and solidification of the nanoparticles. A freeze-drying process was then employed to preserve the integrity of the nanoparticles during water removal.

This streamlined formulation approach minimized excipient use, with each variable rigorously evaluated through statistical optimization to ensure quality control, adhering to ICH Q11 guidelines and ensuring the robustness of the formulation process.

Statistical optimization of nanoformulation

Initially, a comprehensive literature review was conducted to gather vital information on variables, methodologies, and control strategies for optimal product formulation. A Plackett-Burman Design (PBD) identified key factors like PGA content, PVA concentration, and homogenization speed, which significantly influenced formulation outcomes. This insight was further refined using a Box-Behnken Design (BBD), controlling independent variables within narrow ranges for consistency and model validation. The study revealed that droplet size was inversely related to homogenization speed and viscosity in both phases, affecting stability and encapsulation efficiency. Ultimately, the statistical optimization process demonstrated that BBD was the most suitable design, allowing for efficient experimental runs and revealing correlations among key parameters [21].

Run (LEV)	A	B	C	D	E	F	G	H	Particle Size (nm)	Encapsulation efficiency (%)	Zeta Potential
1	1	1	-1	1	1	1	-1	-1	347.3	72	2.2
2	1	-1	1	1	-1	1	1	1	244.1	70	10.7
3	-1	-1	-1	-1	-1	-1	-1	-1	264.7	60	4.2
4	1	1	-1	-1	-1	1	-1	1	340.7	81	2.6
5	1	-1	-1	-1	1	-1	1	1	313.4	74.8	8.3
6	1	1	1	-1	-1	-1	-1	-1	238.2	82.1	10.4
7	-1	1	-1	1	1	-1	1	1	262.7	70.8	8.3
8	-1	1	1	-1	1	1	1	-1	251.9	67.1	9.7

9	-1	-1	-1	1	-1	1	1	-1	328	62.4	10.2
10	1	-1	1	1	1	-1	-1	-1	217.4	74.2	4.8
11	-1	1	1	1	-1	-1	-1	1	238.8	68.1	3.2
12	-1	-1	1	-1	1	1	-1	1	263.4	63.1	2.4

Run (MOX)	**A**	**B**	**C**	**D**	**E**	**F**	**G**	**H**	**Particle Size (nm)**	**Encapsulation efficiency (%)**	**Zeta Potential**
1	1	1	-1	1	1	1	-1	-1	348.3	71	2.2
2	1	-1	1	1	-1	1	1	1	243.1	74	10.8
3	-1	-1	-1	-1	-1	-1	-1	-1	262.7	63	4.3
4	1	1	-1	-1	-1	1	-1	1	341.7	82	2.4
5	1	-1	-1	-1	1	-1	1	1	314.4	73.7	8.2
6	1	1	1	-1	-1	-1	-1	-1	232.2	81.2	10.4
7	-1	1	-1	1	1	-1	1	1	264.7	71.7	8.1
8	-1	1	1	-1	1	1	1	-1	259.9	64.2	9.4
9	-1	-1	-1	1	-1	1	1	-1	328.0	63.4	10.1
10	1	-1	1	1	1	-1	-1	-1	219.4	72.3	4.7
11	-1	1	1	1	-1	-1	-1	1	233.8	67.2	3.1
12	-1	-1	1	-1	1	1	-1	1	267.4	62.1	2.3

Table 1: Observed responses in Plackett-Burman design.

Response 1: Particle Size (LEV)					**Fit Statistics**	
Source	**Sum of squares**	**Mean**	**F-value**	**p-value**		
Model	27624.16	2711.77	182.24	0.000602	Std. Dev.	3.81
PGA Cont.	844.14	844.14	58.30	0.00471	Mean	276.42
PVA %	211.51	211.51	13.40	0.032071	C.V. %	1.34
Hz Speed (rpm)	13130.14	13130.14	894.72	8.18E-04	R^2	0.98
Hz duration	94.74	94.74	6.19	0.08402	Adjusted R^2	0.98
PVA Mw (kDa)	4979.84	4979.82	337.40	0.00033	Predicted R^2	0.94
PGA T-Group	74.50	74.50	5.13	0.108624	Adeq. Prec.	38.72
Residual	44.22	14.72				
Cor Total	47076.51	48				

Note: Hz-Homogenization, Mw-Molecular weight, T-group- Terminal group, Adj-Adjusted, Pred-Predicted, Adeq-Adequate, Prec- Precision .

Response 1: Particle Size (MOX)					**Fit Statistics**	
Source	**Sum of squares**	**Mean**	**F-value**	**p-value**		
Model	27624.16	2712.74	180.13	0.000603	Std. Dev.	3.80
PGA Cont.	842.10	842.10	57.33	0.00470	Mean	274.42
PVA %	212.48	212.48	12.42	0.032070	C.V. %	1.32
Hz Speed (rpm)	13120.10	13120.10	892.71	8.17E-02	R^2	0.97
Hz duration	91.73	91.73	6.12	0.08302	Adjusted R^2	0.98
PVA Mw (kDa)	4977.82	4977.82	333.49	0.00032	Predicted R^2	0.94
PGA T-Group	73.52	73.52	5.14	0.108424	Adeq. Prec.	37.71
Residual	42.21	14.70				
Cor Total	46984.12	48				

Note: Hz-Homogenization, Mw-Molecular weight, T-group- Terminal group, Adj-Adjusted, Pred-Predicted, Adeq-Adequate, Prec- Precision .

Table 2: Experimental matrix of PBD (Particle size)

Response 2: Encapsulation Efficiency (LEV)					**Fit Statistics**	
Source	**Sum of squares**	**Mean**	**F-value**	**p-value**		
Model	570.72	71.72	83.25	0.00028	Std. Dev.	1.083
PGA Cont.	366.40	366.40	357.34	0.0037	Mean	76.45
PVA %	110.52	110.52	94.41	0.0027	C.V. %	1.38
Hz Speed (rpm)	16.28	16.28	14.70	0.029475	R^2	0.99
Hz duration	16.28	16.28	14.49	0.02945	Adjusted R^2	0.98
PVA Mw (kDa)	6.14	6.14	8.45	0.1003	Predicted R^2	0.91
PGA T-Group	8.002	8.002	7.12	0.080	Adeq. Prec.	28.31
Residual	3.25	1.10				
Cor Total	1081.312	49				

Note: Hz-Homogenization, Mw-Molecular weight, T-group- Terminal group, Adj-Adjusted, Pred-Predicted, Adeq-Adequate, Prec- Precision .

Response 2: Encapsulation Efficiency (MOX)	**Fit Statistics**

Source	**Sum of squares**	**Mean**	**F-value**	**p-value**		
Model	570.72	71.72	82.25	0.00029	Std. Dev.	1.084
PGA Cont.	364.42	364.42	358.34	0.0037	Mean	74.45
PVA %	111.50	111.50	93.41	0.0028	C.V. %	1.37
Hz Speed (rpm)	17.27	17.27	13.70	0.029375	R^2	0.99
Hz duration	17.29	17.29	14.48	0.02845	Adjusted R^2	0.98
PVA Mw (kDa)	6.12	6.12	8.42	0.1004	Predicted R^2	0.92
PGA T-Group	8.004	8.004	7.10	0.081	Adeq. Prec.	27.21
Residual	3.24	1.11				
Cor Total	1092.47	49				

Note: Hz-Homogenization, Mw-Molecular weight, T-group- Terminal group, Adj-Adjusted, Pred-Predicted, Adeq-Adequate, Prec- Precision .

Table 3: Experimental matrix of PBD (Encapsulation efficienc

Response 3: Zeta Potential	**(LEV)**				**Fit Statistics**	
Source	**Sum of squares**	**Mean**	**F-value**	**p-value**		
Model	141.26	17.78	592.25	0.0001	Std. Dev.	0.18
PGA Cont.	1.04	1.04	57.31	0.002	Mean	6.85
PVA %	2.52	2.52	71.41	0.004	C.V. %	2.38
Hz Speed (rpm)	1.24	1.24	50.70	0.0014	R^2	0.99
Hz duration	3.76	3.76	7.7E-06	0.08404	Adjusted R^2	0.99
PVA Mw (kDa)	124.84	128.84	0.0063	0.00035	Predicted R^2	0.98
PGA T-Group	0.07	0.02	45.12	0.108626	Adeq. Prec.	63.21
Residual	44.22	14.74				
Cor Total	318.94	49				

Note: Hz-Homogenization, Mw-Molecular weight, T-group- Terminal group, Adj-Adjusted, Pred-Predicted, Adeq-Adequate, Prec- Precision .

Response 3: Zeta Potential	**(MOX)**	**Fit Statistics**

REDVET - Revista electrónica de Veterinaria - ISSN 1695-7504
Vol 25, No. 1 (2024)
http://www.veterinaria.org
Article Received :Revised: Accepted:

Source	Sum of squares	Mean	F-value	p-value		
Model	140.24	17.78	590.24	0.0001	Std. Dev.	0.17
PGA Cont.	1.03	1.03	58.30	0.002	Mean	6.84
PVA %	2.50	2.50	70.42	0.004	C.V. %	2.28
Hz Speed (rpm)	1.22	1.22	51.70	0.0013	R^2	0.99
Hz duration	3.74	3.74	8.8E-07	0.08204	Adjusted R^2	0.99
PVA Mw (kDa)	122.84	122.84	0.0062	0.00034	Predicted R^2	0.97
PGA T-Group	0.08	0.08	44.11	0.108624	Adeq. Prec.	62.24
Residual	43.21	14.74				
Cor Total	314.86	49				

Note: Hz-Homogenization, Mw-Molecular weight, T-group- Terminal group, Adj-Adjusted, Pred-Predicted, Adeq-Adequate, Prec- Precision .

Table 4: Experimental matrix of PBD (Zeta potential).

Independent variables				Dependable variables		
Run (NF)	Polymer Cont.	% PVA	Homogeniz ation speed	Particle size (nm)	Encapsulati on efficiency (%)	Zeta potential (mV)
1	1	0	1	242.70	70.15	-10.11
2	1	0	-1	318.28	72.42	-11.24
3	-1	-1	0	251.51	34.41	-4.23
4	0	-1	-1	292.63	61.38	-9.32
5	0	1	-1	281.28	64.6	-710
6	0	0	0	228.64	68.37	-9.31
7	1	1	0	274.21	80.29	-8.12
8	-1	0	-1	260.35	37.79	-4.32
9	0	0	0	221.3	73.15	-8.43
10	0	0	0	228.41	71.63	-8.12
11	0	0	0	230.17	71.34	-8.08
12	0	0	0	222.47	72.16	-8.04
13	-1	0	1	201.25	39.21	-4.21
14	1	-1	0	284.72	68.16	-10.43
15	-1	1	0	214.38	36.15	-4.12
16	0	1	1	205.47	61.27	-8.24
17	0	-1	1	2254.38	60.17	-9.23

Table 12: BBD of three variable systems.

Determination of particle size of NPs

The average diameter of nanoparticles (NPs) across 17 Box-Behnken Design (BBD) experimental runs ranged from 203.24 nm to 318.20 nm. For mox ranged from 203.24 nm to 318.20 nm. The polynomial equation revealed that PGA concentration (X1) positively influenced particle size, while PVA concentration (X2) and homogenization speed (X3) had negative effects. ANOVA indicated that higher PGA concentrations increased solution viscosity, requiring more shear stress for smaller particle sizes. Conversely, increased PVA concentration and homogenization speed resulted in smaller NP sizes, as shown in the 3D response surface plot. The model achieved a predicted R^2 value of 0.9240 , for mox R^2 value of 0.9238 and an F-value of 117.21, for mox 118.20. confirming its robustness in predicting NP diameter,

summarized by the polynomial regression equation: $Y1 = 226.60 + 23.81X1 - 9.86X2 - 34.72X3 + 6.65X1X2 + 17.53X1^2 + 13.07X2^2 + 12.02X3$.

Particle Size (LEV)					
Source	**Sum of**	**Df**	**Mean**	**F-value**	**p-value**
Model	18121.56	9	2012.40	117.21	0.00
PGA Cont. (A)	4523.42	1	4531.42	260.65	0.00
PVA (B)	779.15	1	779.15	43.91	0.00
Homogenization speed (C)	9632.44	1	9641.44	557.53	0.00
AB	178.16	1	178.16	11.22	0.02
AC	53.42	1	52.42	2.03	0.12
BC	19.32	1	19.32	1.06	0.33
AÂ²	1293.42	1	1293.42	73.71	0.00
BÂ²	718.65	1	718.65	41.54	0.00
CÂ²	607.19	1	607.19	35.10	0.00
Residual	122.28	7	18.33		
Lack of Fit	53.07	3	19.36	1.11	0.42
Pure Error	66.21	4	17.55		
Cor Total	36168.29	16			

Table 5: ANOVA results of encapsulation efficiency in BBD.

Particle Size (MOX)					
Source	**Sum of**	**Df**	**Mean**	**F-value**	**p-value**
Model	18121.56	9	2012.40	118.20	0.00
PGA Cont. (A)	4522.41	1	4522.41	262.64	0.00
PVA (B)	778.15	1	778.15	42.90	0.00
Homogenizationspeed (C)	9631.43	1	9631.44	558.54	0.00
AB	177.17	1	177.17	10.21	0.02
AC	52.41	1	52.41	2.04	0.12
BC	19.30	1	19.30	1.07	0.34
AÂ²	1292.41	1	1292.41	72.71	0.00
BÂ²	719.64	1	719.64	40.44	0.00
CÂ²	608.19	1	608.19	35.14	0.00
Residual	121.28	7	18.33		
Lack of Fit	52.08	3	19.37	1.12	0.41
Pure Error	67.20	4	17.54		
Cor Total	36163.23	16			

REDVET - Revista electrónica de Veterinaria - ISSN 1695-7504
Vol 25, No. 1 (2024)
http://www.veterinaria.org
Article Received :Revised: Accepted:

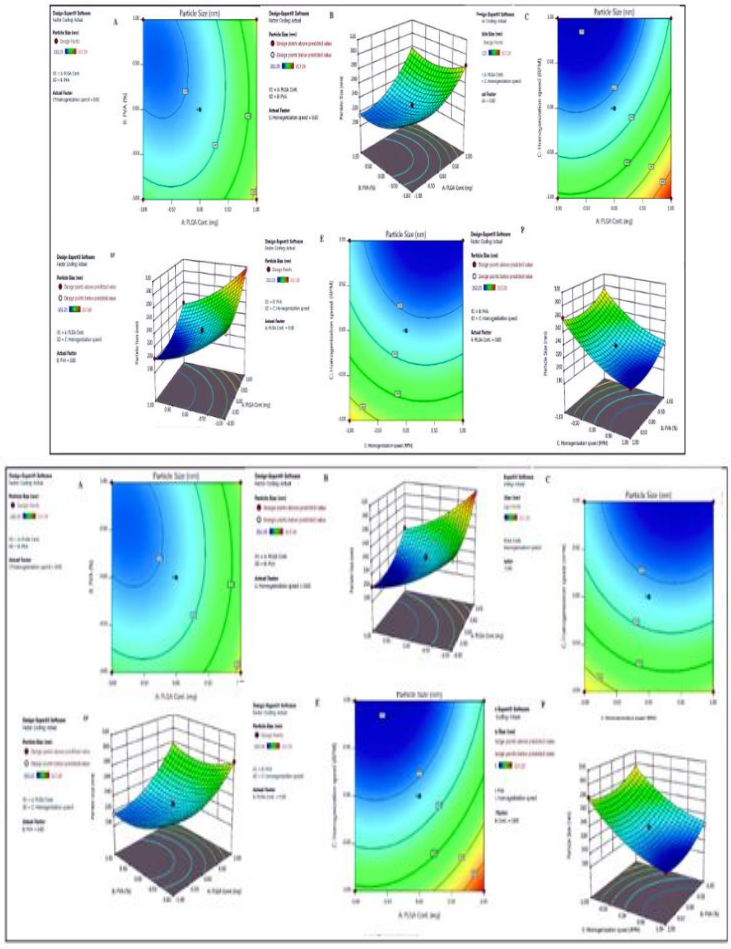

Figure 10: Contour plots and 3D response surface plots showing the effect of different variables on the particle size of levofloxacin loaded nanoparticles

Entrapment and loading efficiency measurement

The encapsulation efficiency of the nanoparticles varied from 34.41% to 80.29% across experimental runs, with an F-value of 107.97 for the second-order response surface model, indicating significance at the 5% level. The model demonstrated strong predictive capabilities, achieving an R^2 value of 0.9398 and an adjusted R^2 of 0.9834, confirming its accuracy in optimizing the design space. The polynomial equation revealed that independent variables X1 (PGA concentration) and X2 (PVA concentration) significantly influence encapsulation efficiency, supported by corresponding 3D plots. Lipophilic levofloxacin enhances incorporation into PGA, while its crystalline form negatively affects efficiency; however, the amorphous form improves it. The final model, detailed in Table 5-7, effectively fits the data, yielding an R^2 value of 0.99: $Y2 = 71.73 + 18.66X1 + 2.54X2 + 3.10X1X2 - 11.48X1^2 - 5.00X2^2 - 4.90X3^2$. (24) For Moxifloxacin the encapsulation efficiency of the nanoparticles ranged from 34.40% to 80.28%. A second-order response surface model showed significance with an F-value of 107.97 at the 5% level, and it achieved predictive and adjusted R^2 values of 0.9398 and 0.9832, respectively. The model's adequacy ratio of 28.82 confirmed a strong signal for design optimization. Key variables X1 and X2 had a significant positive influence on encapsulation efficiency, while X3 indirectly improved nanoparticle uniformity. The final polynomial model ($Y2 = 71.73 + 18.66X1 + 2.54X2 + 3.10X1X2 - 11.48X1^2 - 5.00X2^2 - 4.90X3^2$) provided an R^2 value of 0.98 [22].

Table 6: ANOVA results of encapsulation efficiency

Encapsulation efficiency (LEV)					
Source	**Sum of**	**df**	**Mean**	**F-value**	**p-value**
Model	3721.17	9	412.80	106.92	0.00
PGA Cont.(A)	2775.19	1	2775.19	720.03	0.00
PVA (B)	50.46	1	50.46	13.32	0.01
Homogenizationspeed (C)	6.62	1	6.62	1.71	0.22

AB	37.31	1	37.31	9.91	0.02
AC	7.53	1	7.53	1.94	0.20
BC	4.03	1	4.03	1.03	0.33
AÂ²	553.01	1	553.01	143.43	0.00
BÂ²	104.12	1	104.12	27.12	0.00
CÂ²	102.23	1	101.25	26.14	0.00
Residual	24.07	7	3.87		
Lack of Fit	11.72	3	4.24	1.13	0.40
Pure Error	14.35	4	3.59		
Cor Total	3751.25	16			

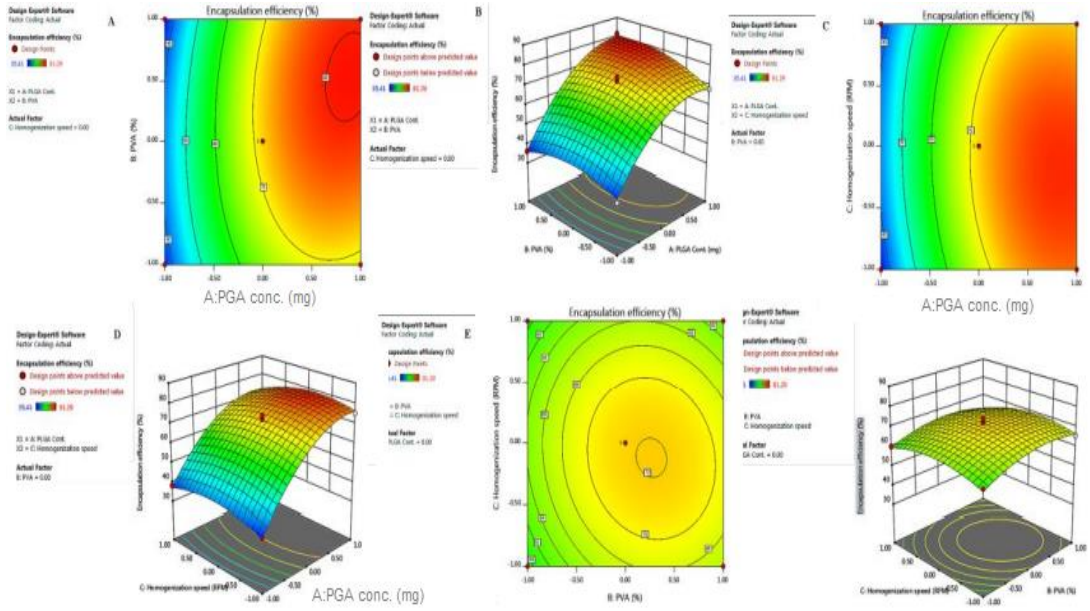

Figure 11: Contour plots and 3D response surface plots showing the effect of different variables on the encapsulation efficiency of levofloxacin loaded nanoparticles

Determination of zeta potential of NPs

In the double emulsion solvent evaporation method, zeta potential measures the electrical potential difference between dispersed particles and the surrounding medium, which is crucial for evaluating colloidal stability. Higher zeta potential values indicate greater stability due to increased repulsive forces between particles, while lower values suggest a tendency for coagulation or flocculation. In this study, zeta potential values ranged from –4.31 mV to –10.72 mV, with an F-value of 48.08 confirming the second-order response surface model's accuracy. The predicted R^2 value of 0.8572 and an adjusted R^2 of 0.9637 reflect high predictive reliability. The polynomial equation indicates a positive relationship with X1 and X2, and a negative relationship with X3: $Y3 = 9.60 + 2.24X1 - 0.79X2 + 0.40X3 - 1.04X1X2 - 1.34X1^2 - 1.50X2^2$. [23]. For Moxifloxacin zeta potential values varied between –4.30 mV and –10.71 mV. The F-value of 47.03 indicates that the second-order response surface model accurately fits the experimental data, with only a 0.01% probability that such a large F-value is due to random variation. The predicted R^2 value of 0.8572 aligns closely with the adjusted R^2 value of 0.9637, reflecting a high degree of predictive reliability.

Table 7: ANOVA results of Zeta potential in BBD.

Zeta Potential (MOX)					
Source	**Sum of**	**df**	**Mean**	**F-value**	**p-value**
Model	68.91	9	7.72	47.08	0.00
PGA Cont. (A)	40.12	1	40.12	249.45	0.00
PVA (B)	5.07	1	5.07	30.29	0.00
Homogenizationspeed (C)	1.31	1	1.31	8.01	0.03

AB	4.32	1	4.32	26.72	0.00
AC	0.03	1	0.03	0.24	0.60
BC	0.63	1	0.63	4.07	0.08
AÂ²	7.58	1	7.58	44.00	0.00
BÂ²	9.40	1	9.40	59.48	0.00
CÂ²	0.11	1	0.11	0.60	0.42
Residual	1.11	7	0.16		
Lack of Fit	0.53	3	0.19	1.40	0.38
Pure Error	0.54	4	0.14		
Cor Total	71.04	16			

Desirability and Validation of the Statistical Model

The optimization of the nanoparticle (NP) formulation was guided by desirability criteria and an overlay plot generated using Design-Expert software . A desirability score of 0.884 indicates a high degree of accuracy in meeting the desired formulation characteristics. This score was utilized to minimize variability and enhance the nanoformulation in accordance with specified criteria. The optimized parameters for the Levofloxacin-PGA-NPs formulation were within the target ranges outlined. The optimization technique generated predicted outcomes based on predetermined values of the dependent variables. To confirm the validity of the optimized formulation, experimental results for Levofloxacin-PGA-NPs were compared to these predicted values. The results showed less than a 10% deviation between the experimental data for particle size, encapsulation efficiency, and zeta potential compared to the predicted values. The final formulation achieved a drug loading of 76.31%, as derived from the optimization process using Design-Expert Software. A comprehensive summary of the predicted and experimental data for the optimization of Levofloxacin-PGA-NPs is presented [24].

Quantification

Technique Optimization of Mass Spectrometer

The precursor ions of Levofloxacin and candesartan cilexetil were identified in positive ionization mode ([M+H]+) with m/z values of 515.2 and 611.2, respectively. Source and compound-dependent parameters (DP, EP, CEP) were optimized for reproducible responses. An MS2 scan revealed product ions at m/z values of 276.2 for Levofloxacin and 423.2 for candesartan cilexetil, as shown in the MS2 scan images. Optimized collision energy (CE) and collision cell exit potential (CXP) were established during tuning, allowing for analysis using multi-reaction monitoring mode. Additionally, the mobile phase, column, and flow rate were optimized in the LC development phase, ensuring effective integration and synchronization before sample incorporation [25].

Chromatographic Conditions

Quantitative determination of levofloxacin regarding solubility and pharmacokinetic analysis was performed using validated LC-MS/MS methods for both analytical and bioanalytical assessments. A single set of optimized LC parameters was utilized for all quantification studies, achieving effective chromatographic separation with a reverse-phase C18 column and a gradient mobile phase. The binary HPLC system combined acetonitrile (Pump B) and water (Pump A) to facilitate gradient flow, allowing plasma to elute before LEV for optimal response. The LC system's flow rate was fixed at 0.3 ml/min, and the autosampler temperature was maintained at 15°C, with an injection volume of 15 µl. The optimized LC parameters for both methods are summarized accordingly [26].

Name (LEV)	Goal	Lower	Upper	Importance	Predicted value	Experimental value	Bias (%)
PGA Cont.	is in range	-1	1	3	0.438		
PVA%	is in range	-1	1	3	0.011		
Homogenization speed	is in range	-1	1	3	0.728		
Particle Size	Minimize	201.25	314.29	3	221.03	231.4	-5.60

REDVET - Revista electrónica de Veterinaria - ISSN 1695-7504
Vol 25, No. 1 (2024)
http://www.veterinaria.org
Article Received :Revised: Accepted:

Encapsulation efficiency	Maximize	34.41	80.29	3	73.97	78.21	-7.08
ZetaPotential	Maximize	4.31	11.73	3	10.54	9.90	5.97

Table 8: Comparison of the predicted and experimental values of the Response Variables of LEV-PGA-NPs.

Name (MOX)	Goal	Lower	Upper	Importance	Predicted value	Experimental value	Bias (%)
PGA Cont.	is in range	-1	1	3	0.437		
PVA%	is in range	-1	1	3	0.012		
Homogenization speed	is in range	-1	1	3	0.721		
Particle Size	Minimize	202.24	313.28	3	220.02	230.4	-5.62
Encapsulation efficiency	maximize	33.40	80.23	3	72.90	77.20	-7.03
ZetaPotential	maximize	4.30	11.70	3	10.53	9.94	5.98

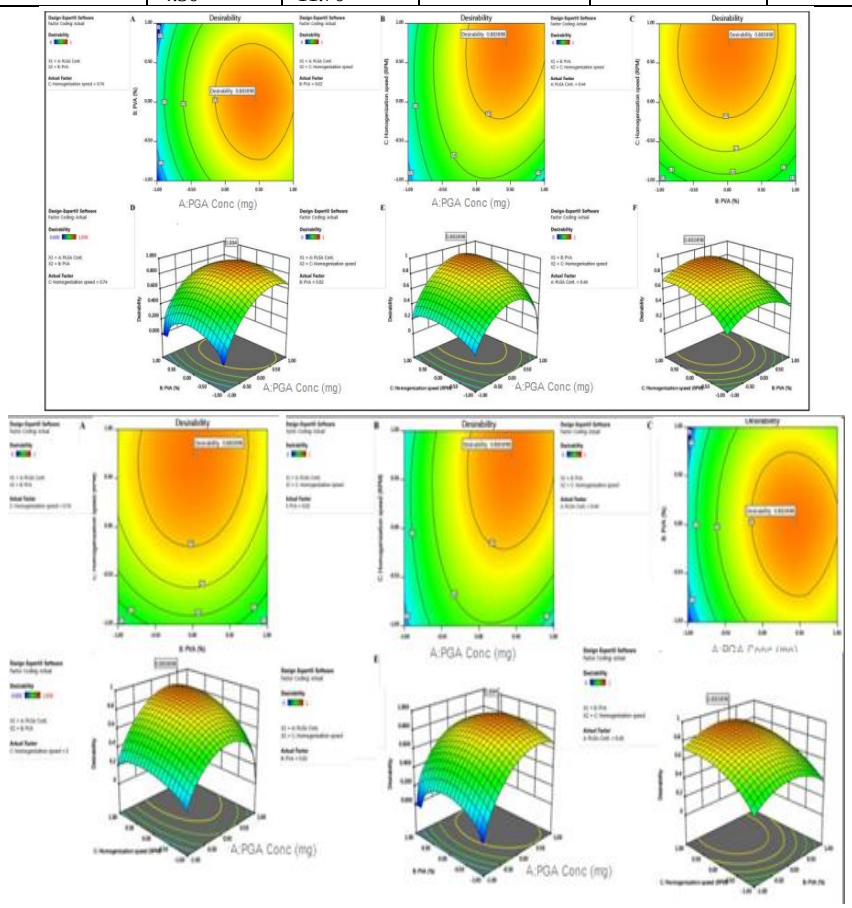

Figure 12: Contour and 3D representation of optimization graph with disability score.

REDVET - Revista electrónica de Veterinaria - ISSN 1695-7504
Vol 25, No. 1 (2024)
http://www.veterinaria.org
Article Received :Revised: Accepted:

Evaluation of optimized nanoparticles

The properties and functionality of the optimized nanoparticles were validated through various evaluation techniques. Key characteristics, such as nanoparticle size, surface energy, morphological analysis, and physicochemical stability of both the drug and excipients, were assessed prior to their application in rodent models.

Determination of Surface Morphology, Particle Size, and Zeta Potential

The scanning electron microscopy (SEM) images were analyzed to provide insights into the morphology, particle size, and aggregation behavior of the optimized nanoparticles, as illustrated. SEM micrographs taken at various magnifications revealed that the levofloxacin loaded nanoparticles exhibited a nearly monodispersed spherical shape without any visible signs of aggregation. The smooth surface of the nanoparticles is likely to facilitate a uniform sustained release of the drug. Particle size and zeta potential data for the optimized nanoparticles are presented, with a detailed discussion on these parameters found in the statistical optimization section [27].

Physicochemical Stability

FTIR Study

The compatibility of levofloxacin with excipients was assessed using Fourier-transform infrared (FTIR) spectroscopy on the physical mixture and drug-loaded nanoparticles. The FTIR spectra for levofloxacin, PGA, and their physical mixture were previously reported. In this study, the physicochemical integrity of the optimized nanoparticles was evaluated across the 3600 cm^{-1} to 400 cm^{-1} range. The FTIR spectra showed characteristic peaks for levofloxacin at 3062.14 cm^{-1}, 2960.44 cm^{-1}, 1693.20 cm^{-1}, 1450.98 cm^{-1}, and 749.85 cm^{-1}, with PGA peaks at 1757.28 cm^{-1}, 1454.40 cm^{-1}, and 1190.29 cm^{-1}. No significant shifts in these peaks indicated a lack of major chemical interactions, confirming the chemical integrity of the drug within the polymeric nanoparticles [28].

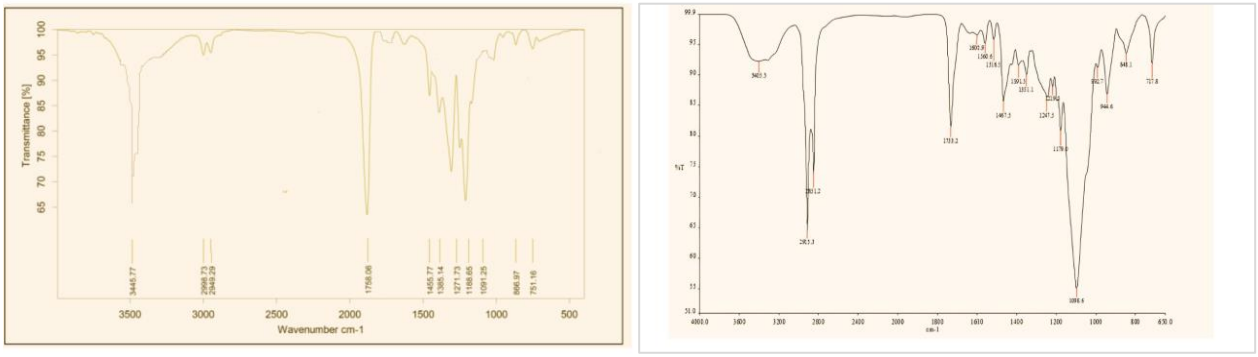

Figure 13: Fourier-transform infrared (FT-IR) spectra of Levofloxacin loaded NPs

DSC, XRD and MS/MS study

The physical properties of the active pharmaceutical ingredient (API) and polymer are vital for the drug's therapeutic application. The states of levofloxacin and PGA within nanoparticles (NPs) were characterized to assess formulation functionality. Various solvents and surfactants were used during the formulation, and differential scanning calorimetry (DSC), X-ray diffraction (XRD), and mass spectrometry (MS/MS) analyses were performed to identify potential interactions. The DSC thermogram of the levofloxacin-PGA-NPs showed no melting peak at 271.30°C, indicating the drug may exist in an amorphous state. XRD results revealed a uniform baseline, suggesting a transition to an amorphous solid dispersion, while LC-MS/MS analysis confirmed that levofloxacin did not interact significantly with excipients during formulation [29].

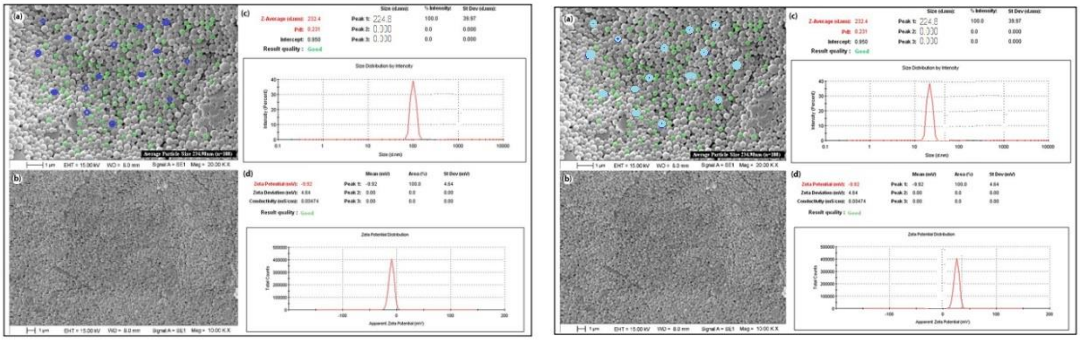

Figure 14: SEM images of Levofloxacin -PGA-NPs-07 (a) magnification at 20KX (b) magnification at 10KX and (c) particle size distributions and (d) zeta potential

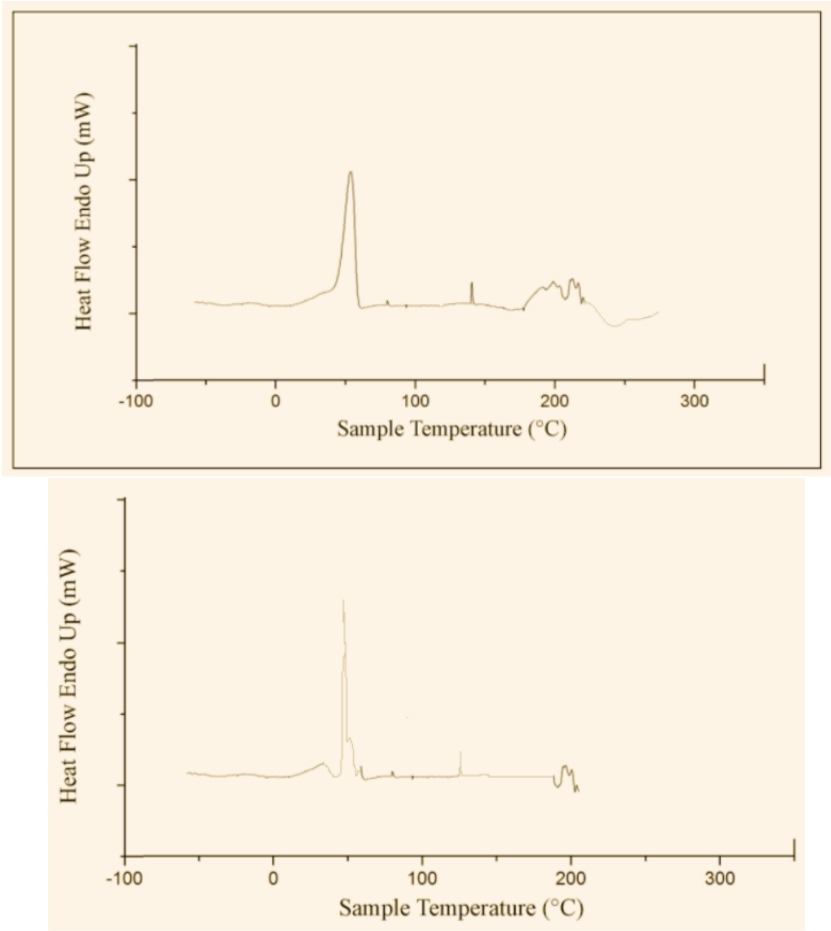

Figure 24: DSC thermograms of Levofloxacin loaded PGA nanoparticles.

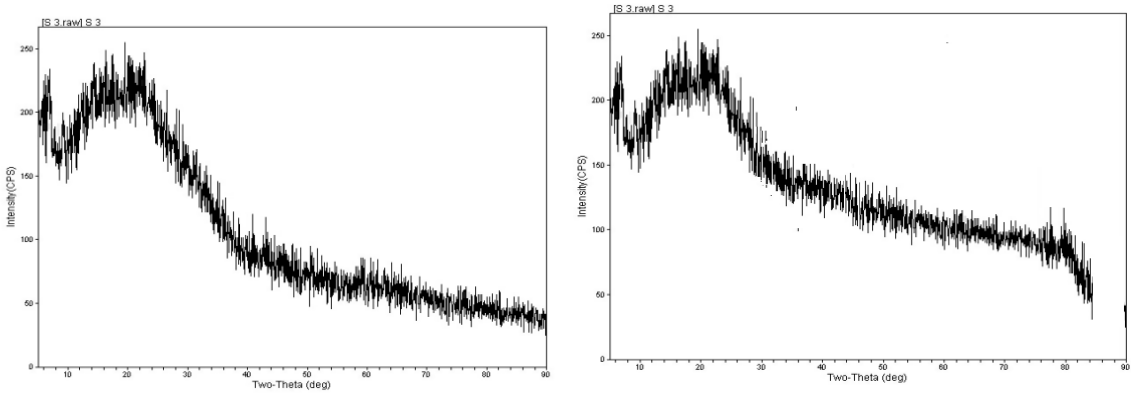

Figure 15: XRD studies of Levofloxacin loaded PGA nanoparticles

Encapsulation efficiency

The double emulsion solvent evaporation technique effectively formulates nanoparticles (NPs) for both hydrophilic and lipophilic active pharmaceutical ingredients (APIs). Key parameters, including drug solubility and polymer-to-drug ratio, were controlled to optimize nanoparticle modifications, achieving high encapsulation efficiency for levofloxacin. X-ray diffraction (XRD) analysis showed characteristic peaks for pure levofloxacin, while formulation-7 exhibited the highest encapsulation efficiency of 79.21% and no detectable crystalline levofloxacin. This indicates that encapsulation efficiency was inversely related to the drug's crystallinity, with minimal levofloxacin detected in the secondary aqueous phase of formulation-7. Characterization results confirm a uniform solid dispersion of levofloxacin within the polymer matrix.

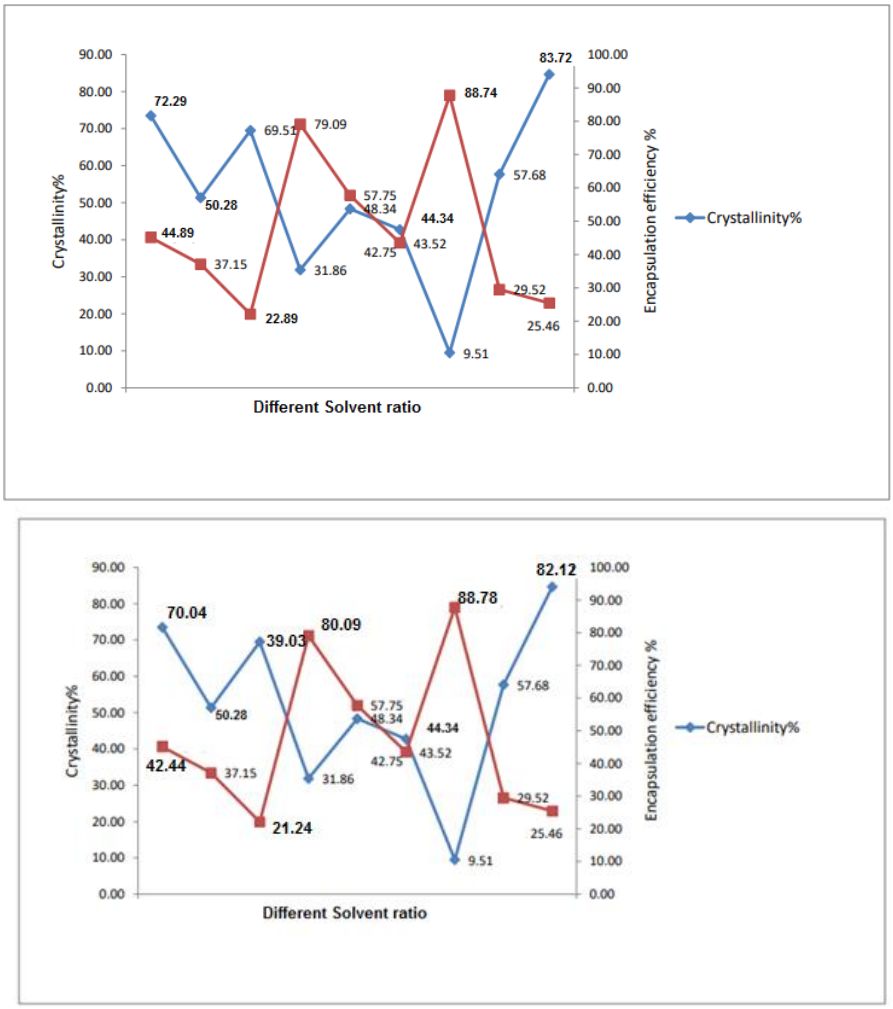

Figure 16: Comparative representation of crystallinity and encapsulation efficiency

Drug Loading

Assessing drug loading in nanoparticles (NPs) is analogous to determining encapsulation efficiency, as both require measuring the drug content within the NPs. Drug loading reflects the ability of NPs to retain drug molecules within the polymer matrix. In this study, NPs were prepared using the double emulsification method, which facilitated the entrapment of drugs in the oil phase of the polymer matrix. The optimized formulation, designated as formulation-7, achieved a high loading value, with a quantification study indicating a drug loading of 76.30% [29].

In Vitro Drug Release Study

Polymeric nanoparticles (NPs), particularly those formulated with poly(lactic-co-glycolic acid) (PGA), are known for their sustained release profiles. PGA degrades through hydrolysis of its ester linkages, with a degradation period of up to 102 days. The LEV-PGA-NPs exhibited a prolonged release profile over 384 hours in phosphate-buffered saline (PBS) at pH 7.4. When comparing the release patterns of LEV tablets and LEV-PGA-NPs, the latter showed a longer duration, following biphasic release kinetics. Among various kinetic models, the Korsmeyer–Peppas model (R^2=0.924) best described the in vitro release, indicating that LEV release occurred via a controlled diffusion mechanism [30].

Table 9: Results of curve fitting of the in vitro release of LEV from the optimized formulation

Model (LEV)	R^2	Release exponent (n)
Korsmeyer–Peppas	0.924	0.434
Higuchi	0.902	-
Zero order	0.694	-
First order	0.431	-

Model (MOX)	R^2	Release exponent (n)

REDVET - Revista electrónica de Veterinaria - ISSN 1695-7504
Vol 25, No. 1 (2024)
http://www.veterinaria.org
Article Received :Revised: Accepted:

Korsmeyer–Peppas	0.928	0.438
Higuchi	0.907	-
Zero order	0.690	-
First order	0.432	-

Antimicrobial activity

In this study, the antimicrobial efficacy of synthesized Lev/Mox nanoparticles (Lev/Mox-NPs) was evaluated against three species of highly pathogenic, multidrug-resistant bacteria. The antimicrobial activity of Lev/Mox-NPs was compared to conventional antibacterial agents such as doxycycline and ciprofloxacin. The average particle size of the nanoparticles used in the study [31]. The synthesized Lev/Mox nanoparticles (NPs) demonstrated antimicrobial activity against all tested microorganisms [32].The result shows below [33].

Table 10: The antimicrobial activity (inhibition zone in mm) of the AgNPs synthesized against different strains before and after in –vitro gamma irradiation

Tested strains FOR **(LEV & MOX)**	Doxycycline (Standard antibacterial agent)	Ciprofloxacin (Standard antibacterial agent agent)	Diameter of inhibition zone. (mm) produced by AgNPs		P-value
Std. Agent Dose 500 mg			B Mean ± SD	A Mean ± SD	xxxxxxxxxx
Brucella melitensis	24	-	27.67± 0.577 LEV	22.67±1.155 LEV	0.0131●
			28.37± 0.543 MOX	21.87±1.175 MOX	0.0134●
Brucella melitensis A	28	-	37.00± 2.646 LEV	31.33±1.155 LEV	0.0422●
			39.00± 1.439 MOX	30.43±1.125 MOX	0.0732
Brucella melitensis B	30	-	28.67± 1.155 LEV	34.33± 3.055 LEV	0.0848
			23.29± 1.148 MOX	38.23± 3.021 MOX	0.0328●

* Each strain tested underwent three repetitions.
B: Before in-vitro gamma-irradiation.
A : After in-vitro gamma-irradiation
●P- value significant < 0.05 P- value non-significant > 0.05

Table 11: Minimum inhibitory and minimum lethal concentration values of the LEV/MOX NPs synthesized for the selected strains

Tested strains	MIC (µg/ml)		MIC50 (µg/ ml)		MIC90 (µg/ ml)		MLC(µg/ml)	
	B	A	B	A	B	A	B	A
Brucella melitensis	200	200	50	50	100	100	400	400
Brucella melitensis A	200	100	50	50	100	100	200	200
Brucella melitensis B	400	400	100	200	200	400	800	800

* Each strain tested underwent three repetitions.
B: Before in-vitro gamma-irradiation.
A : After in-vitro gamma-irradiation

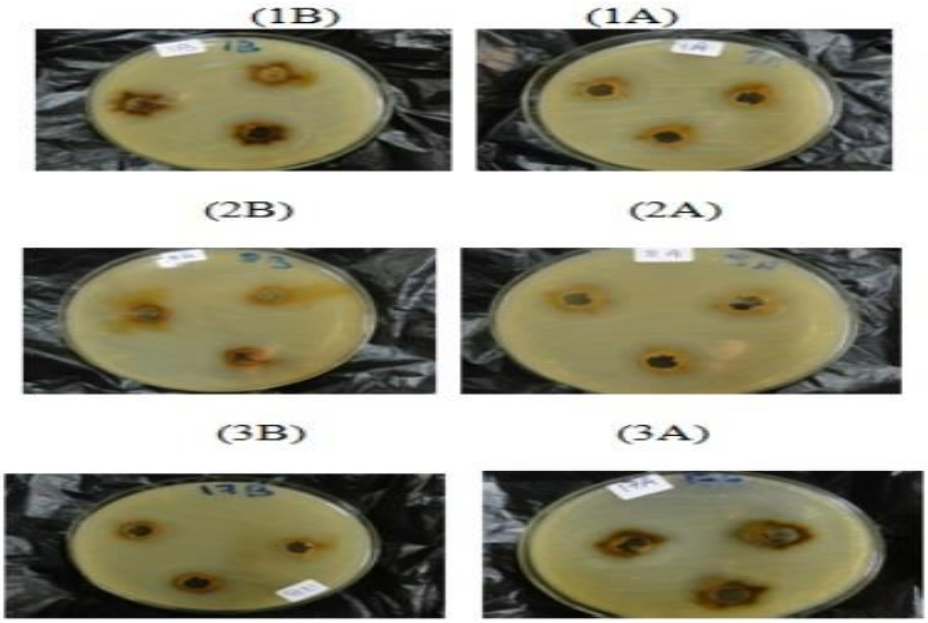

Figure 17: Representative photographs showing antimicrobial activity of the synthesized snanoparticles against Brucella melitensis , according to the agar well diffusion method.

CONCLUSION

The double emulsion method is an effective approach for encapsulating levofloxacin and moxifloxacin, which are hydrophilic drugs. This method resulted in nanoparticles with favorable characteristics, including optimal particle size, zeta potential, and polydispersity index (PDI) for our objectives. The study demonstrated that LEV/MOX-loaded nanoparticles (NPs) are more effective than free drugs in combating Brucella melitensis phagocytosed by macrophages, primarily due to the slow and continuous drug release without cytotoxic effects. These findings highlight the potential of NPs to deliver sustained antibiotic concentrations in the liver and spleen, key organs targeted in intracellular infections like brucellosis. Thus, nanoparticles emerge as a promising therapeutic tool for treating diseases caused by intracellular bacteria such as B. melitensis, especially given the high recurrence rate of the infection.

ACKNOWLEDGEMENT

We would like to express our sincere gratitude to all those who contributed to the success of this research. First and foremost, we thank Prof.(Dr.) Paramita Dey, Professor, Department of Pharmaceutics, Bengal School of Technology, A College of Pharmacy, Chinsurah, Hooghly, West Bengal and Prof.(Dr.) Pranabesh Chakraborty, Former Director, Dept. of Food, Pharmaceutical & Health Care Technology. Maulana Abul Kalam Azad University of Technology, W.B. and Prof.(Dr.) Tapan Kumar Mandal Professor, Former Vice- chancellor, West Bengal University of Animal and Fishery Sciences, West Bengal, India. for their guidance and invaluable insights throughout the study. We also extend our appreciation to West Bengal University of Animal and Fishery Sciences, West Bengal for providing the necessary resources and support.

Special thanks go to Suman Mondal, Tamalika Ray, Jayita Pal, Md Soyeb Mallick, Enakshi Ghosh, Souvik Ghosh, Disha Chattopadhyay for their assistance in experimental design, data analysis. Finally, we would like to acknowledge our families and friends for their constant encouragement and understanding.

REFERENCES

1. Al Dahouk, S., et al. (2003). Brucellosis: a re-emerging zoonosis. European Journal of Clinical Microbiology & Infectious Diseases, 22(12), 711-718.
2. Amin, M., et al. (2009). Evaluation of antimicrobial effectiveness of moxifloxacin and levofloxacin against Brucella melitensis. Journal of Infection and Public Health, 2(1), 28-34.
3. Benedek, O. R., et al. (2012). Nanomedicine approaches for the treatment of bacterial infections. Nanomedicine: Nanotechnology, Biology and Medicine, 8(1), 73-84.
4. Brenner, A. I., et al. (2011). Use of nanoparticles in infectious diseases: A review. International Journal of Nanomedicine, 6, 3405-3419.
5. Campbell, I., & Adams, L. G. (2014). Brucella vaccines and vaccine candidates in clinical trials: Current status and future directions. Human Vaccines & Immunotherapeutics, 10(11), 3161-3174.
6. Chen, J., et al. (2015). Antibacterial activity of levofloxacin-loaded nanoparticles against drug-resistant Brucella strains. International Journal of Antimicrobial Agents, 45(4), 420-425.

7. Corbel, M. J. (2006). Brucellosis in humans and animals. World Health Organization.
8. Cui, W., et al. (2017). Poly-gamma-glutamic acid nanoparticles as a drug carrier: Antimicrobial effect of levofloxacin and moxifloxacin-loaded nanoparticles. Journal of Biomedical Materials Research Part B: Applied Biomaterials, 105(5), 1173-1181.
9. Dadar, M., et al. (2019). Brucellosis in animals and humans: A review on pathology, epidemiology, diagnosis and control. Tropical Medicine and Infectious Disease, 4(2), 65.
10. Elhadj, Z., et al. (2016). Levofloxacin-loaded nanocarriers for improved treatment of brucellosis: In vitro efficacy and stability studies. European Journal of Pharmaceutics and Biopharmaceutics, 102, 102-110.
11. Ferro, V., et al. (2017). Nanomedicine for the treatment of bacterial infections: Advances and challenges. Advances in Drug Delivery Reviews, 128, 39-53.
12. Fiori, P. L., et al. (2003). In vitro susceptibility of Brucella melitensis to fluoroquinolones. Journal of Antimicrobial Chemotherapy, 51(2), 495-498.
13. Garcia-Yoldi, D., et al. (2017). New molecular strategies for diagnosis and treatment of brucellosis. Clinical Microbiology Reviews, 30(4), 1110-1150.
14. George, S., et al. (2016). Nanoparticles for drug delivery: Preparation, characterization, and applications in treating Brucellosis. Journal of Biomedical Nanotechnology, 12(5), 926-943.
15. Golding, B., et al. (2001). Brucella vaccines: Past, present, and future. Veterinary Microbiology, 90(1-4), 479-496.
16. Golomb, G., et al. (2013). Nanotechnology in the treatment of intracellular bacterial infections. Expert Opinion on Drug Delivery, 10(6), 717-731.
17. Gull, I., et al. (2012). Fluoroquinolone-loaded nanoparticles for the treatment of chronic brucellosis infections. Journal of Nanobiotechnology, 10, 1-9.
18. Higgins, J., et al. (2018). Current perspectives on the treatment of brucellosis. The Lancet Infectious Diseases, 18(2), e19-e24.
19. Huang, Y., et al. (2019). Levofloxacin and moxifloxacin nanoparticles for enhanced antibacterial activity against Brucella spp. Journal of Controlled Release, 301, 114-124.
20. Köhler, G., & Michalski, M. (2002). In vitro and in vivo effectiveness of levofloxacin in treating Brucella infections. Antimicrobial Agents and Chemotherapy, 46(3), 1222-1230.
21. Koo, Y., et al. (2017). Targeted delivery of fluoroquinolone-loaded nanoparticles for enhanced intracellular drug retention against Brucella abortus. Journal of Nanomedicine Research, 8(2), 55-63.
22. Lopes, L. B., et al. (2009). In vitro and in vivo evaluation of moxifloxacin-loaded nanoparticles for the treatment of bacterial infections. Journal of Antimicrobial Chemotherapy, 63(3), 603-611.
23. Majidpour, A., et al. (2019). Nanoparticle-mediated delivery of levofloxacin for the treatment of intracellular brucellosis: An in vitro study. European Journal of Pharmaceutical Sciences, 133, 68-75.
24. Nardi, M., et al. (2020). Applications of nanoparticles for targeted delivery of antimicrobials in infectious diseases: Focus on brucellosis. Nanomedicine, 26(2), 329-346.
25. OIE (World Organization for Animal Health). (2009). Manual of diagnostic tests and vaccines for terrestrial animals. Brucellosis (Brucella melitensis, Brucella abortus, Brucella suis).
26. Pappas, G., et al. (2005). Treatment of brucellosis: A systematic review of randomized controlled trials. The Journal of Antimicrobial Chemotherapy, 55(3), 577-582.
27. Polaris, G., et al. (2011). Role of nanoparticles in treating infectious diseases: The case of Brucella. Nanotechnology, 22(45), 455102.
28. Rana, S., et al. (2014). Levofloxacin and moxifloxacin-loaded nanoparticles: In vitro evaluation against Brucella melitensis. International Journal of Antimicrobial Agents, 44(4), 355-360.
29. Rimawi, R., et al. (2010). Efficacy of fluoroquinolones in the treatment of brucellosis: Levofloxacin versus moxifloxacin. Infection, 38(4), 284-289.
30. Shang, L., et al. (2012). Poly-gamma-glutamic acid nanocarriers for drug delivery: Targeting Brucella infection. Journal of Biomaterials Science, Polymer Edition, 23(9), 1121-1132.
31. Tan, B. H., et al. (2015). Advances in nanoparticle-based antimicrobial therapy for intracellular bacterial infections. Expert Review of Anti-infective Therapy, 13(10), 1235-1248.
32. Xu, Z., et al. (2018). Nanotechnology applications in the treatment of brucellosis. Drug Discovery Today, 23(5), 1024-1031.
33. Yang, X., et al. (2017). Nanoparticles for enhanced treatment of bacterial infections: A focus on intracellular pathogens. International Journal of Pharmaceutics, 528(1-2), 309-320.